Memoirs of the Faculty of Engineering, Kyushu University, Vol.71, No.2, June 2011

Human Impacts on Erosion and Deposition in Onga River Basin, Kyushu, Japan

by

Tu Anh TRAN[*], Yasuhiro MITANI[**], Hiro IKEMI[***]
and Hirotada MATSUKI[†]

(Received May 17, 2011)

Abstract

Human disturbances on the ground surface cause erosion and deposition in difference types of landscape. Research on erosion and deposition will understand the magnitude of these impacts in the past and now. In this paper, sediment volume stored in channel for long-term (Holocene) is calculated and erosion model (RULSE) is applied to estimate erosion in short-term (few decades). These values are compared with the one of denudation model established in Japan. As a result, it has clarified that an amount of 47% of total sediment yield from denudation is discharged to the channel for long-term sediment storage in Onga River basin. The RULSE model has indicated that 48% of the total sediment yield comes from erosion processes as sheet and rill erosions, and 52% comes from mass movement such as slope failure. Currently, the sediment yield from forest and agriculture activities is considered to be about 69,000 ton/year which is higher consists of 28% of long-term annual erosion for whole basin.

Keywords: Holocene, Sediment storage, Erosion, Land-use, Human impact, Denudation

1. Introduction

To understand what the human do act on geomorphological processes such as erosion and deposition in the period without human impact, some researchers have reconstructed the past environment, as sediments stored in ponds or small reservoirs, or store/erosion in catchments, and sediments discharge out of basins.

In Japan, Oguchi (1996) commented that very rapid erosion can occur under natural conditions without human disturbances. Sedimentation rate was 1.14 m per 1000 years since 20 ka, based on ^{14}C ages (Akojima, 1983), 1.0 m per 1000 years on average in Holocene (Yamanoi, 1986), and 0.4

[*] PhD. Candidate, Department of Civil and Structural Engineering
[**] Associate Professor, Department of Civil and Structural Engineering
[***] Assistant Professor, Department of Civil and Structural Engineering
[†] Director, Himeji office of River and Road, Kinki Regional Development Bureau, MLIT, Japan

m per 1000 years (Oguchi, 1997). Syvitski et al. (2005) predicts the flux of sediment on a river-by-river basis under modern conditions and before human influence in global scale. The results show that global sediment flux increases strongly in the basin without reservoirs over pre-human or anthropogenic loads. In small scale, Hoffman et al. (2007) used sediment budget to calculate the rates of alluvial sediment and erosion during the Holocene. He found that 50% of Holocene alluvial sediment is deposited along the trunk valley and the delta (Rhine River in German) while the rest is stored along the tributary valleys. Rommens et al. (2001) estimated that 50% of the sediment eroded during Holocene was stored in colluvial deposits as foot slopes and dry valley bottom, and another 29% of sediment mass is stored in the alluvial plain in the catchment size of 50 km^2.

For sediment load and discharge, sediment loads in present days are 1.6 times greater than those in about 30 million years ago (Tardy et al., 1989). Lemons (1995) compared the erosion rate in Late Pleistocene to modern time in Weber River that sediment yield value is about two times higher than modern basins of similar sizes in USA.

It doesn't clear that the current erosion is over or under 'natural value' due to the lack of long-term record (Holocene) of sediment transport for river in most area of the world (Walling, 1999). An attempt to analyse the covers occupied by forest and cultivate was established to derive an approximate the magnitude of the increasing sediment yield related to land disturbance by human activities (Dedkov and Mozzherin, 1984). Some researches only consider the sediment discharge out of the basin due to lacking of stored sediment in the drainage system or hill slope.

In this paper, we focus on the sediment storage and erosion of the Onga River basin, Japan, as a study area. At first, we estimate sediment storage and erosion in the study area for long time (over thousands of years). Then, we compare that with current erosion to estimate the magnitude of sediment yield related to the human disturbance on the land-cover.

2. Onga River Basin

2.1 Location and geology

Onga river basin located in the northern Kyushu Island, covers 1036 km^2 with average discharge is 18.4 m^3/s. The highest elevation is 1180 m in the south east of the basin. The channels are almost U-shape. The Onga River basin consists of 69.2% rock before Quaternary (hard rock) and 30.8% Quaternary sediment (almost soft soils). Based on 50m-grid and hydrogical analysis using Geographic Information System (GIS), the Onga River has maximum stream order 8 as definition of Strahler (1957), and 1- 2 orders are covered by the catchment size less than 0.5km^2, which has nearly no Quaternary deposit as shown in Geological map. According to the stream order, the Onga River basin can be divided into three main sub-catchments include Miyawaka area, Iizuka and Tagawa area (**Fig.1**).

Quaternary deposits include most of the Late Pleistocene sediments belong to Wakamatsu formation in the estuary of the basin. This formation consists of two members Shozugahama mud, and Iwaya sand and gravel members. The Shuzugahama mud (2m thick) is exposed along the coast composed of silt with small amount of pebble and sand. The Iwaya sand and gravel member (15-20m) made up mainly of pebble gavel and sand with silt (Ozaki et al., 1993).

In this area, there are many tephra such as Kikai-Akahoya (K-ah), aged 6300 years BP, occurs in marine deposits (Machida, 1991); AT (AIRA – Tn tephra) which is dated around 21 – 22 ka years BP; and Aso-4 tephra (70 ka years BP).

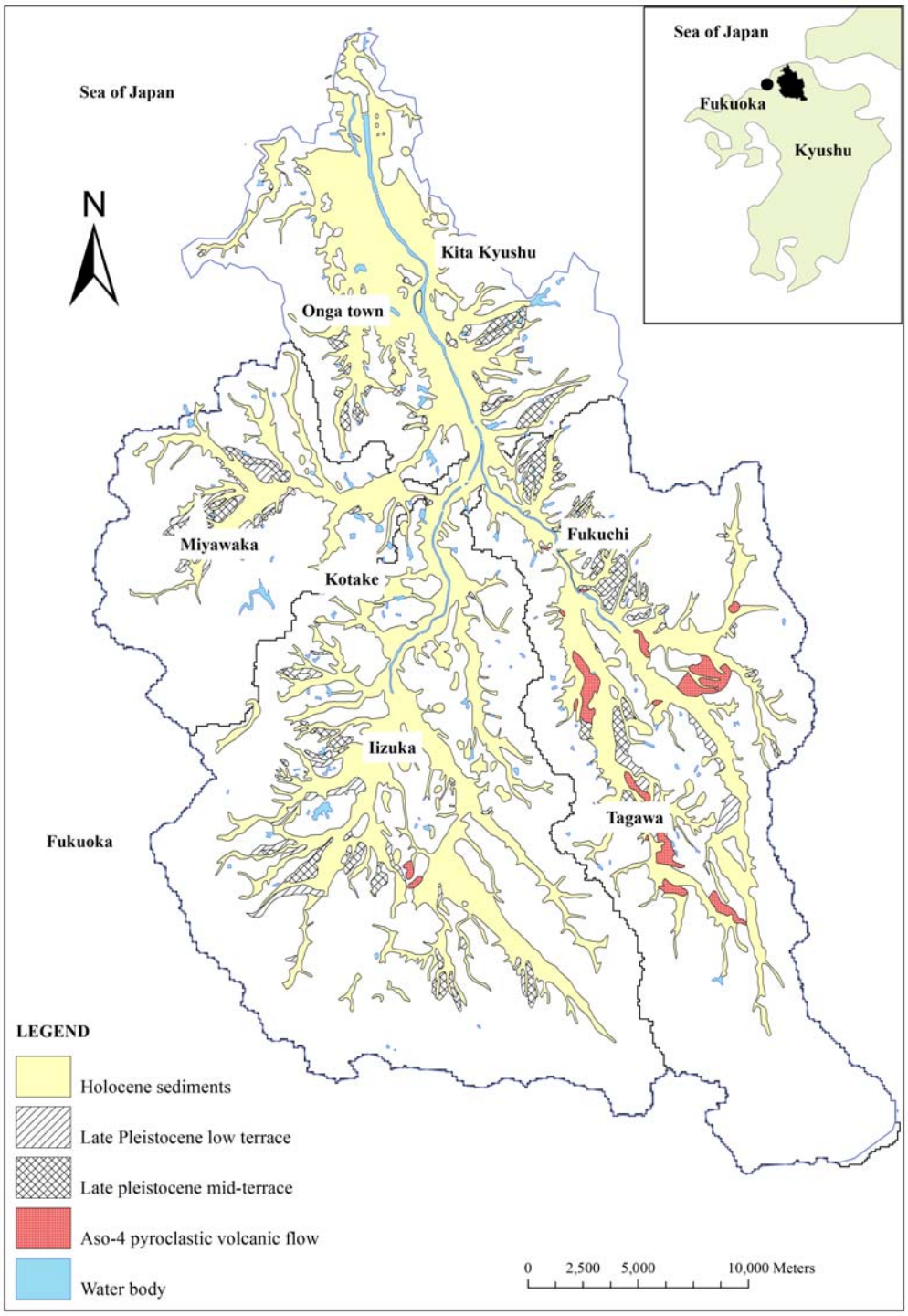

Fig.1 Onga River basin and sub-catchments shown on geological base map (modified from Tran et al., 2010a)

2.2 Sea level change in Quaternary

Sea-level changes in Late Pleistocene-Holocene played a very important role to form the sediment along the coastal plain (Matsubara, 2000). During the Last interglacial transgression or Shimo-sueyoshi transgression, the sea level rose at peak in 130-120 ka years BP, near present sea level in the northern Kyushu (Kaizuka, 1980), and was at -7.9 ± 1.5 m in Onga, north-western Kyushu (Shimoyama et al., 1999). In the Last Glacial age, 20 -15 ka years BP, the sea level drop -140 to -120 m and reached the lowest peak at around 18 ka years BP in comparison with today's one (Kaizuka, 1980 & Yasuda, 1990). In Late-glacial, 13 ka – 10 ka years BP, the sea level increased to -10m lower than that of today one, which formed the sea sediments contained a lot of shells at around below -15 m and gravel layer from -10 to -14m (Tran et al., 2010a). And then, the sea level withdrew to -40 m around 11 ka to 10 ka years BP to form the coarse grain size along the seashore (Umitsu, 1991). For example, 10 m thickness pebble in Hakata bay (Karakida et al., 1994), which underlies by fine grain size; and about 5 meter sand without shells in Onga River mouth. Another example, two channels are recognized with the lowest at -20 m and another at about -18 m which correspond to sea level dropped in early Holocene, prior it increased gradually to maximum in mid Holocene. From 10000 years BP to 8000 years BP, the rate of sea level rise was slower than that was in the period of 8000 years BP to 6500 years BP (1.5 to 2.0 cm/year). A research in Fukue, an island located about 200 km to the southwest of Onga River, showed that the mean sea level is above -11.4 m at about 7900 years BP. From 8000 years BP to 5000 years BP, mean sea level rose with an average speed of 0.40 cm/year (Yokoyama, 1996). The sea-level rose to maximum around 6000 year BP (Umitsu, 1991) or Jomon transgression. We assume that the bottom of Holocene sediment in the Onga plain has been formed around 8500 years BP.

In the late Jomon period, around 6000 years BP, the sea level was higher than that is in present 2 to 3 meter (Karakida et al., 1994) to maximum +4.0m in the northern Kyushu (Pirazzoli, 1991), that made Onga village area become the lagoon and caused the major deposition of the Hakata member (Karakida et al., 1994). In this period, most of marine sediments deposit to form the silt layer in Onga town area (Tran et al., 2010a). Then, minor sea-levels dropped have been recognized in 5000-4000 years BP and 3000-2000 years BP (Umitsu, 1991).

3. Sediment Storage in the Onga River Basin

3.1 Surface interpolation of Pleistocene – Holocene

There are two kinds of Holocene and Pleistocene boundaries needed to define. The first is the boundary of Holocene and pre-Holocene on the surface, which is easily defined in the geological map 1:200,000 published by Geological Survey of Japan, and the second is the boundary in the strata or in vertical section as mentioned below.

Total 393 boreholes, pass through the Holocene sediment, are used to define the Holocene boundary, which have attributes as depth of bedrock, the thickness of mud/silt layer, shell mounds, volcanic ash inter-bed silt layers, grain sizes. The types of sediment are different in lowland and upper parts of the river basin, so that different methods are used to define the boundary in two areas.

In Onga river plain, 17 boreholes in different sites appear volcanic ash (A-Kh) and a lot of boreholes contain the shell fragments. Therefore, Shimoyama et al. (1999) have described that the silt layer in Onga town (Onga river silt layer) belongs to Holocene (Geological Society of Japan, 2010). Machida et al. (1991) have shown that the K-ah thickness is about less than 20 cm, AT ash thickness is 50 cm (Nakada & Lambeck, 1998). Otherwise, there are a lot of tephra of Aso-4 flows in the upper reaches of the study area. The thickness of volcanic ash changes from 0.4 m to 0.8 m

which inter-bed in marine deposits at about -7 m to -8 m depth, and up to 1 m in other deposits. The Aso-4 tephra interrupted when the sea level drop between Obaradai and Misaki transgressions (Machida, 1991) and AT formed when the sea level was lowest, so they may not appear in the marine silt layer. Tran et al. (2010a) assume that the volcanic ash within the marine deposits is K-ah, and the others should be AT, Aso-4 or older.

To define this surface in upper reaches, the sediment-comparison between Late Pleistocene terraces and borehole data, and the grain size changes in the borehole, especially, the silt/clay layers is done. There are two main cycles of sedimentation, markedly, the first silt layer is about 4 m to 5 m and N-value (from standard penetration test) is less than 0-5, and the silt layer should be deposited when the sea level rise in Holocene. Another should be formed when the sea level rise in Late Pleistocene (Tran et al., 2010a).

Stream order and catchment are extracted from digital elevation model (DEM), 50 m resolution published by Geospatial Information Authority of Japan (GSI) by using GIS. The order number is directly proportional to relative watershed dimensions, and channel size at that place in the system and two drainage basins differing in linear scale can be compared with respect to corresponding point in their geometry. A given order catchment contains all the streams of its system ended at its maximum order, for example, 5 order catchment will contains its stream network and extent to the end of 5 order stream where it meets another stream at the same or higher level (junction).

It is found that almost the riverbeds of stream order less than 4 expose the bedrock. In addition, the stream order 5, 6 and 7 have U-shape valley which is used to predict the value at where lacks of data. In the results, the negative and abnormal values have been checked to modify by fieldwork (Tran et al., 2010b). Based on sea level change, tepra in combination with borehole analysis, the bottom of Holocene surface in Onga plain is assumed to 8500 year BP, when sea level rose to form the marine sediment from -14 m to -15 m, and fixed with stream order 8.

There are three main methods to interpolate a surface such as Inverse Distance Weighted (IDW), Spline and Kriging. The Spline method is an interpolation method that estimates values using a mathematical function that minimizes overall surface curvature, resulting in a smooth surface that passes exactly through the input points. IDW is a method of interpolation that estimates cell values by averaging the values of sample data points in the neighborhood of each processing cell. The closer a point is to the center of the cell being estimated, the more influence, or weighted, it has in the averaging process. Kriging method based on statistical models that include autocorrelation—that is, the statistical relationships among the measured points (ESRI, 2007). Depend on the type or/and characteristic of data, one or more methods are used to give a best surface. In this case, there are limited data, steepness valleys, and the outputs must pass exactly through the input points. The Spline method Tension, controls the stiffness of the surface according to the character of the modeled phenomenon, gives the best surface as expected.

3.2 Sediment storage estimation

Sediment storage or sediment deposition in the catchment in Holocene is calculated from two surfaces, Holocene surface and current surface. Almost sediments are stored in the plain of catchments of 6 and 7, but there is less or no sediment deposited in stream of catchment lower 5. The sediment thickness in Holocene is shown in **Fig.2**.

Tran et al. (2010a) proposed a relationship between catchments area and storage volumes for Holocene period (10000 years):

$$y = 10^{-3}(0.7x - 5), \quad (1)$$

where,

y is the volume of sediment in [km^3],

x is the catchment area in [km^2].

If the time span of deposition is 8500, eq.(1) will be

$$Y = y/8500 = 84\times10^{-9}\,(x - 7.1) \qquad [\text{km}^3/\text{year}]$$

or

$$Y = 84\,(x - 7.1) \qquad [\text{m}^3/\text{year}] \qquad (2)$$

This formula is used to calculate the sediment discharge rate in comparison with sediment yield in the drainage basin, and can be used to estimate sediment volume of the catchment areas in the range of 10 to 1000 km^2. On average, the Onga river basin stored 84,000 m^3 sediments per year. Based on geomorphology at the Onga river estuary, there is a sand bar formed in Late Pleistocene located in front of the Onga plain which consists almost Holocene sediment. Because a lagoon formed in the early-mid Holocene when the sea level rose, most of sediments from upstream could strongly deposit.

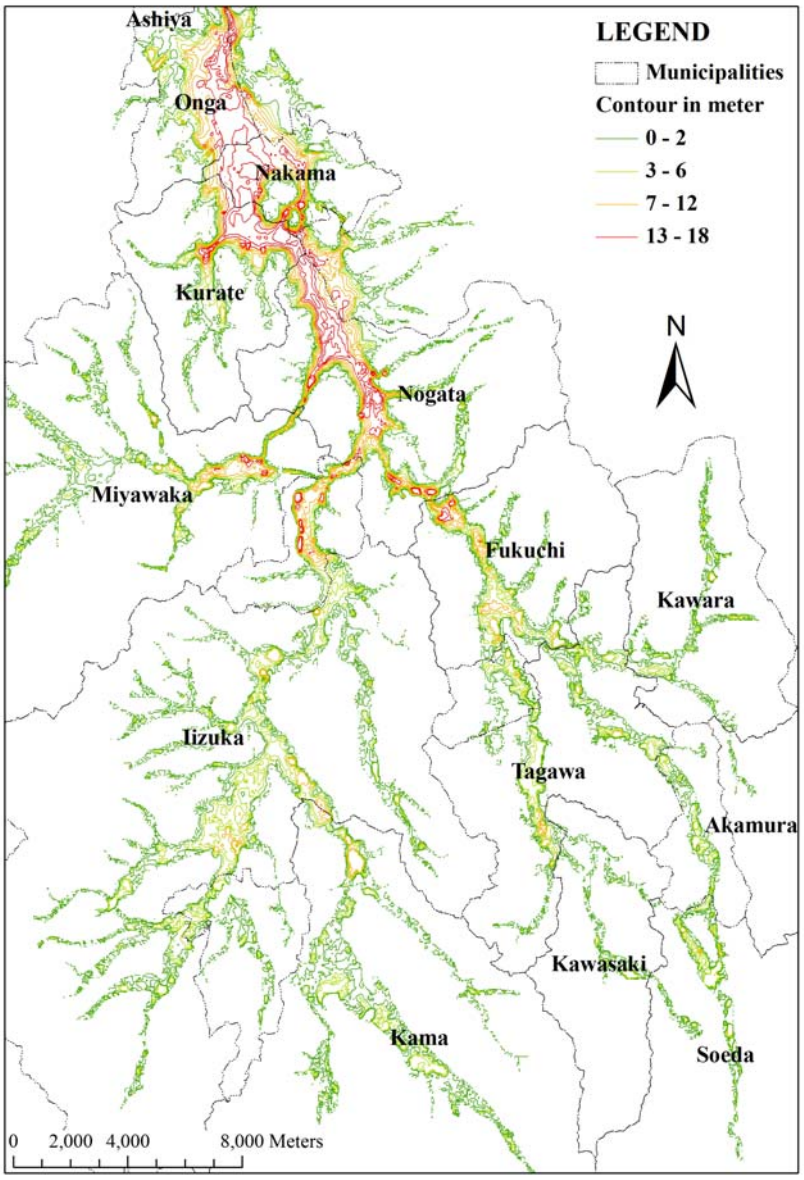

Fig.2 Spatial distribution of the Holocene sediment thickness (modified from Tran et al., 2010b).

4. Erosion in the Onga River Basin

4.1 Denudation model

There is no exact definition for long-term sediment yield, but almost authors mention about over thousands years. Long-term sediment yield was calculated by different methods as proposed by Oguchi (1996, 1997, 2001), Yamamoto (2005), Wilkinson (2009), Trimble (1981), Church (1989), Rommens et al. (2006), etc. In Japan, Ohmori (2003) proposed that the denudation rate is proportional with elevation. His model bases on 82 reservoirs throughout Japan which have sediment volume over 50,000 m^3, storage capacity over 2,000,000 m^3, sedimentation ratio to water storage capacity less than 25%, and observation duration longer than 10 years, with longest duration of 66 years. Most of these reservoirs are located in the upper-most of the catchment in a sequence of reservoirs through individual rivers, in which the erosion is considered as a natural process less affected by human activities. He also proved that the model can be applied for a drainage basin (open system) and a long-term period (ten thousands years or longer), and for drainage basin area larger than some tens of km^2.

$$E = \alpha D^{\beta} \qquad \text{[mm/year]} \qquad (3)$$

where,

α and β are constants (α=4.4x10^{-5}; β=2.2),

E is *denudation* rate, in [mm/year],

D (dispersion of *altitude*) is the standard deviation:

$$D = \left[\frac{\sum_{i=1}^{n} (h_i - H)^2}{n-1} \right]^{1/2} \qquad \text{[m]} \qquad (4)$$

In which, H is the mean altitude given by:

$$H = \frac{\sum_{i=1}^{n} h_i}{n} \qquad \text{[m]} \qquad (5)$$

This model is used to estimate sediment yield in the catchment.

4.2 RULSE model

The Revised Universal Soil Loss Erosion (RUSLE) originated from Universal Soil Loss Equation (USLE) is an erosion model designed to predict the short-term (few decades) average soil loss in the disturbance of human as land-use, which widespread applied in the world. In Japan, modified USLE have been used and its parameters were also modified by Taneda (1980). After that, many authors tried to apply this model in some parts of Japan, in the farmland area (Yoshikawa et al., 2004 and Shiono, et al., 2002), forest area and steep slopes (Kitahara et al., 2000). The model consists of 6 factors as below:

$$A = R \times K \times LS \times C \times P \qquad (6)$$

where,

K is a quantitative description of the inherent erodibility of a particular soil; it is a measure of the susceptibility of soil particles to detachment and transport by rainfall and runoff, expressed in [t·h·MJ^{-1}·mm^{-1}],

R is based on kinetic energy considerations of falling rain (Whelan, 1980) and represents a measure of the erosive force and intensity of rain in a normal year (Goldman et al., 1986), expressed in [MJ·ha^{-1}·h^{-1}·year^{-1}·mm^{-1}],

L is the slope length (non-unit),

S is the slope steepness (non-unit),

C is the land cover (non-unit),

P is the practice management (non-unit).

4.2.1 Soil erodibility factor (*K*)

This factor (t·h·MJ^{-1}·mm^{-1}) is estimated from the soil sample test result (from National Institute for Agro-environmental Sciences) and soil map in scale 1:200,000 of Fukuoka prefecture. There are total 9 soil types in the soil map (**Table 1**). *K* was calculated from the formula as

$$K = \left[2.1 \times M^{1.14} \times 10^{-4} \times (12 - a) + 2.35 \times (b - 2) + 2.5 \times (c - 3)\right] \times 0.1317 \div 100 \qquad (7)$$

where

K in [t·h·MJ^{-1}·mm^{-1}],

M = (%silt + % sand) (100 – %clay),

a is organic matter (%),

b is structure code in **Fig.3** (non-unit),

c is profile permeability class in **Table 2** (non-unit).

Table 1 K-value for each soil type.

Soil group	Symbol	Area km^2	Samples	Range	K-SI
					t·h·MJ^{-1}·mm^{-1}
Brown forest soil	BFS	729.27		0.014-0.024 0.004-0.030[5)]	0.019
Brown lowland soil	BLLS	1.57	3	0.003-0.009	0.005[5)]
Gray lowland soil	GLLS	64.68	35		0.016
+Coarse grain	GLLS-C	21.93	12	0.003-0.02	0.014
+ Fine grain	GLLS-F	62.64	23	0.009-0.03	0.018
Dark red soil	DRS	8.99	1		0.007
Sand dune, residual	IM	3.49	1		0.002
Gley soil	GL	24.67	15	0.017-0.032	0.022
Peaty soil	PT	9.25	1		0.012
Yellow soil	YS	25.69	7	0.02-0.035	0.024
Kuroboku	AN	0.49	1	0.007	0.006[10)]
Restoration		72.42	1		0.018

K of rice field restoration from mining is given by the value of the soil sample fall in its region. There are five types of BFS from the soil map scale 1:200,000 such as: dry BFS, wet BFS, moist BFS, ryBFS (red yellow), dBFS (dark), which are grouped into BFS (we have the value for only Brow Forest Soils.) due to the lack of detail data. This *K*-value is also referenced from the literatures in Japan. In the soil map, there are three types of gray lowland soils such as coarse grain, fine grain gray lowland soil and gray lowland soil. The first and second were calculated directly from the soil test results, the last is an average of coarse and fine grain types. Sand dune type value is defined based on the same type sample in the other area.

The data from National Institute for Agro-environmental Sciences of Japan includes texture type, and relation between texture and permeability in **Table 2** and **Fig.3.**

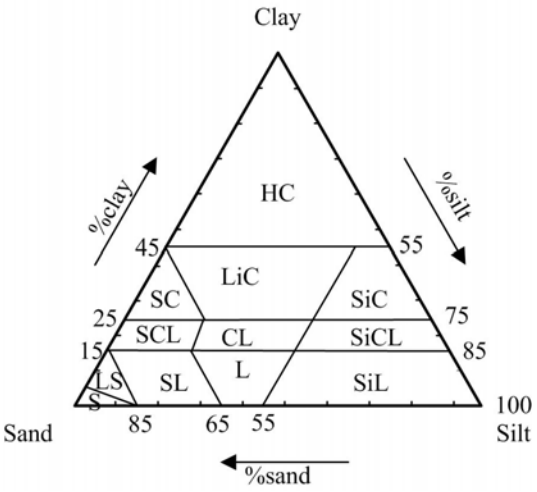

Fig.3 Diagram defines the soil structure in Japan.

Table 2 Permeability code for soil type.

Texture	**Symbol**	**Structure code** (b)	**Permeability code**[9] (c)
Silty clay, clay	SiC, HC	1	6
Silty clay loam, sandy clay	SiCL, SC	2	5
Sandy clay loam, clayey loam	SCL, CL, LiC	2	4
Loam, silty loam	L, SiL	2	3
Loamy sand, sandy loam	LS, SL	2	2
Sand	S	3	1

4.2.2 Rainfall erosivity factor (*R*)

R-value is interpolation base on 9 stations, which have a distance between 17 km. The rainfall data is recorded in 10 minutes intervals from 1995 to 2010 from AmeDAS (Japan Meteorological Agency-JMA) and in 60 minutes intervals before 1995.

A break between storms is defined as 6 hours or more with less than 1.3 mm of precipitation. Rains less than 13 mm, and separated from other storms by 6 hours or more, are omitted as insignificant unless the maximum 15 minutes intensity exceeds 24 mm·h^{-1}. (Wischmeier and Smith, 1978). Renard et al, (1993) proposed the modified method to calculate the *R* value as follows.

Rainfall intensity for particular increment of a rainfall event (i_r) is calculated as

$$i_r = \frac{\Delta V_r}{\Delta t_r} \tag{8}$$

where,

Δt_r is the duration of the increment over which rainfall intensity is considered to be constant, expressed in hour,

ΔV_r is the depth of the rainfall (mm) during the increment. If i_r is greater than 76 mm/h, it will be given 76 mm/h.

Rainfall energy per unit depth of rainfall (e_r in [MJ· ha^{-1}·mm^{-1}]) can be calculated as

$$e_r = 0.29\left[1 - 0.72\exp\left(-0.05i_r\right)\right] \quad (9)$$

The total storm kinetic energy (E in [MJ·ha^{-1}·mm^{-1}]) is calculated as:

$$E = \sum_{r=1}^{m} e_r \Delta V_r \quad (10)$$

To calculate the erosion index (EI) value for particular rainstorm ([MJ· ha^{-1}·mm^{-1}·h^{-1}], total storm kinetic energy (E) is multiplied by the maximum amount of rain falling within 30 consecutive minutes (I_{30}) in [mm·h^{-1}].

The average annual rainfall and runoff erosivity factor (R) [MJ·ha^{-1}·h^{-1}·year^{-1}·mm^{-1}] is the average of calculated EI-values and other points where lack of data are linear interpolation. R-values in other location are interpolated by linear method.

$$R = \frac{1}{n}\sum_{j}^{n}\left[\sum_{k}^{m}\left(E\right)_k\left(I_{30}\right)_k\right]_j \quad (11)$$

where,

E is the total storm kinetic energy (MJ·ha^{-1}),

I_{30} is the maximum 30 minute rainfall intensity (mm·h^{-1}),

j is an index of *the* number of year used to produce the average,

k is an *index* of the number of rain storms in each year,

n is the number of years used to obtain the average R,

m is number of rain storm in each year.

Base on 2621 rainfall storms, we establish the relation between $I_{60\max}$ and EI_{30}, the relation as

$$EI_{30} = 0.5664 \cdot I_{60\max}^{2.01} \qquad (r^2=0.891) \quad (12)$$

where,

EI_{30} is the erosion index for particular rainstorm (MJ·mm·ha^{-1}·h^{-1})

$I_{60\max}$ is the maximum amount of rainfall within 60 consecutive minutes (mm·h^{-1}).

This relation can be used to calculate R-value for the station or year of/in which the data is recorded in 60 minute intervals such as rain gauge stations in the study area before 1995.

Taneda (1981) estimated the R-value in Kyushu vary from 2704 to 6683 MJ·mm·ha^{-1}·h^{-1} (276 to 682 as expressed in m^2·tf·ha^{-1}·h^{-1}).

Table 3 R-value [MJ·mm·ha^{-1}·h^{-1}·year^{-1}] in each year from 1990 to 2010.

Year	Munakata	Yahata	Soeda	Minami	Hikosan	Dazaifu	Iizuka	Asakura	Sasaguri
1990	2859	3253	2195	3758	4638	1392	2585	3496	2989
1991	6713	6025	5725	7338	7446	6899	8619	6886	6118
1992	2442	2315	8828	3660	4821	4494	2905	2947	2669
1993	4048	3850	5495	6079	7788	4475	5457	6290	2522
1994	1842	1570	2516	1926	2933	1859	1951	1692	3356
1995	4869	7107	9014	10708	9659	6478	2759	9281	6791
1996	2833	4387	4579	8461	9071	3250	3487	4215	6362
1997	4293	6955	7698	10862	14902	9237	6086	9924	10344
1998	5434	5598	3979	5994	5955	4757	3438	5531	2835
1999	4226	7121	7155	7123	9572	7805	5874	7570	7831
2000	2478	3127	2346	3249	4984	3888	3870	6200	2556
2001	3322	5026	3098	7282	7495	7014	5168	5540	5360

2002	2204	3423	2311	4662	4477	4874	4550	4073	2720
2003	6738	10027	7666	14775	5456	9549	10166	6369	7785
2004	4426	7483	4566	11184	15096	4735	5408	7991	8905
2005	2585	3800	5251	8422	8104	3926	3905	6670	4803
2006	5117	5515	9409	11323	12517	9502	9871	12139	7873
2007	5229	4698	3823	3939	10382	5175	2932	6394	4621
2008	3525	4675	10099	7451	9086	8026	7659	5660	6520
2009	5741	5469	2009	4982	8402	8295	6488	9221	8976
2010							5283	5649	
Ave.	**4046**	**5047**	**5614**	**7159**	**8139**	**5782**	**5165**	**6368**	**5597**

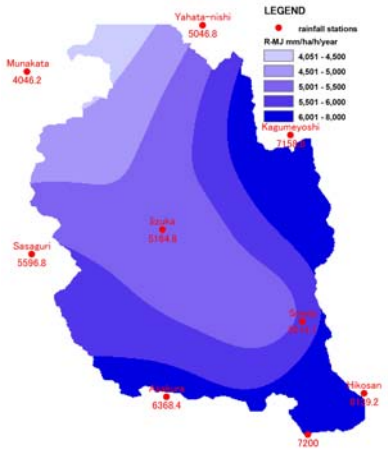

Fig.4 Distribution of *R*-value.

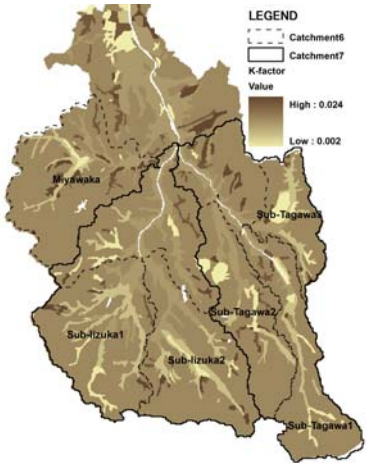

Fig.5 Distribution of *K*-value.

4.2.3 Slope length factor (*L*)

L factor is calculated as (Desmet and Govers, 1996), derived from

$$L = (m+1)\cdot\left(\frac{\lambda}{22.13}\right)^{m} \tag{13}$$

Or assuming that the center of the grid cell is representative for the whole cell, we have:

$$L_{i,j} = (m+1)\cdot\left(\frac{2\cdot A_{i,j-in} + D^2}{2\cdot D\cdot x_{i,j}\cdot 22.13}\right)^{m} \tag{14}$$

where, $L_{i,j}$ is the slope length factor in one cell (non-unit),

$A_{ij\text{-}in}$ is the contributing area at the inlet of a grid cell with coordinate (i,j), in [m^2],

$x_{i,j}$ is a factor with accounts for variations in the width of flow resulting from the orientation of the cell with respect to the contour. It has a value of 1.0 when the flow exits over the side and 1.414 when the flow exits over a corner. In this case, this value is given by 1.0, which causes the maximum values in each cell,

m is the length exponent of the USLE *LS*-factor (non-unit), and in this calculation is 0.5[5)4)18)],

D is the cell size, in [m],

$A_{i,j}$ can be calculated by using GIS and DEM.

4.2.4 Slope steepness factor (S)

Many authors mentioned about this values as, McCool et al., (1989).

$$S=10.8\sin\beta + 0.03 \quad \text{if } \tan\beta<0.09 \tag{15}$$

$$S=16.8\sin\beta - 0.50 \quad \text{if } \tan\beta\geq 0.09 \tag{16}$$

or

$$S=\left(\frac{\sin\beta}{0.0896}\right)^{1.3} \tag{17}$$

In Japan, this value is proposed by Agricultural Structure Improvement Bureau[12].

$$S=0.38\cdot e^{0.075\cdot\beta}+0.068 \tag{18}$$

where β is expressed in [degree].

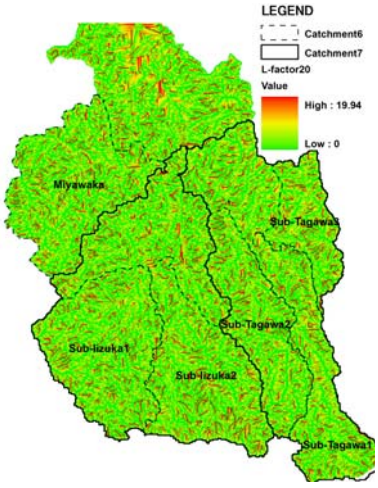

Fig.6 Distribution of L- factor (from eq. (14)).

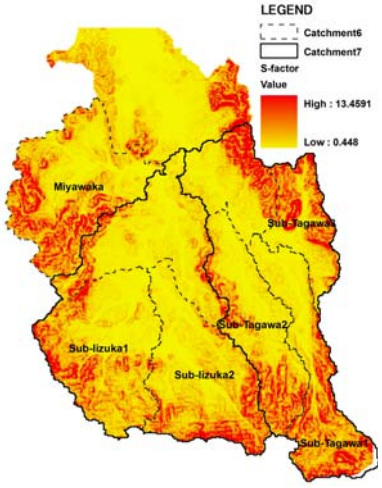

Fig.7 Distribution of S-factor (from eq.(18)).

4.2.5 Cover and Practice factors (CP)

Land-use types are defined based on the land-use map in 1997 published by Counsellor, National and Regional Planning Bureau, Ministry of Land, Infrastructure, Transport and Tourism of Japan. CP values are referred from literatures (**Table 4**). C-values of mining, urban, roads and water bodies are given as zero. C-value of forest type is average of natural and artificial ones.

Table 4 CP-factor from some study cases in Japan.

Type of cover	C	P	Note
Forest	0.01[4]	1	Average of natural and artificial forests
Field	0.34[5][6][10][12] (mean)	0.27[5][6]	1-4°
		0.3	4-7 °
		0.4	7-10 °
		0.45	10-15 °
		0.5	15-25 °
Paddy field	0.02[4]	0.5[4]	
Golf course	0.02[5]	0.17[4]	
Deforestation	0.129[4]	0.23[4]	replaced by planting trees

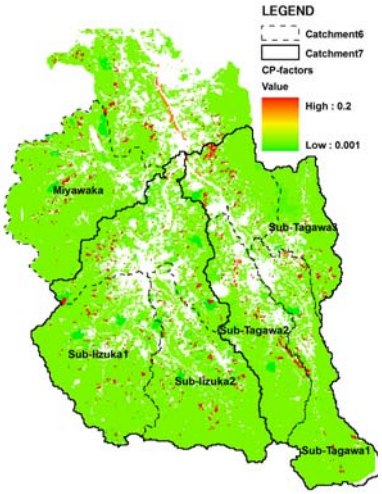

Fig.8 Distribution of CP factor (Table 4).

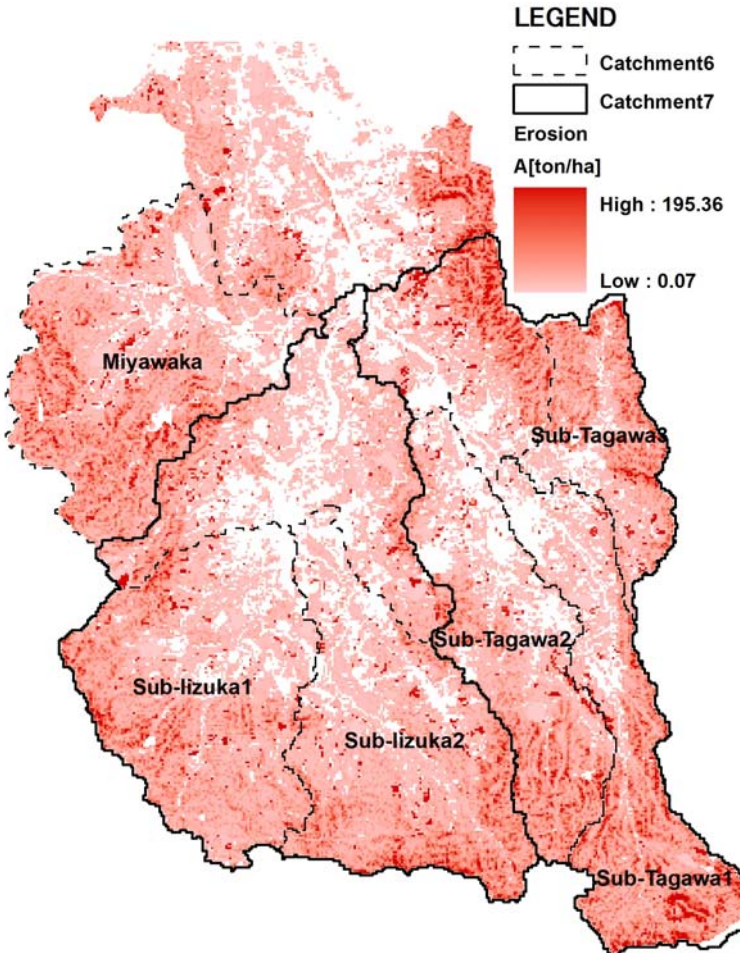

Fig.9 Soil loss map in Onga river basin.

Table 5 Statistic the erosion by land cover.

Type of cover	Ratio %	Total (ton/ha)
Forest	66.89	220,667
Paddy field	23.05	29,363
Field	2.85	50,394
Golf	1.41	242
Deforest	5.80	7,300
Total	**100**	**307,966**

There are two results which are obtained for two areas, whole catchment (A) and forest area (A_{forest}). The result calculated for whole catchment is show in **Fig.9**. Erosion by type of land-use is shown in **Table 5**, and total sediment erosions in each catchment are listed in **Table 7**. There are 171 cells with over 92 ton/ha, or 0.22% which fall into the field areas. Other land-use areas have the erosion value up to 50 ton/ha. In the forest area, CP-value is equal to 0.01 (**Fig.8**) and K-value is 0.019 (**Fig.5**) so that eq.(6) will be

$$A_{forest} = 1.9 \times 10^{-2} \times R \times L \times S \times K \quad (19)$$

or $$A_{forest} = 1.9 \times 10^{-4} \times R \times L \times S \quad (20)$$

A_{forest} can represent erosion without human disturbance or natural erosion of RUSLE.

4.3 Comparison two erosion models

In the forest area, erosion from Ohmori model is E_{forest}, and erosion RULSE model is A_{forest}. We assume that these values are the same because they depend on natural factors. E_{forest} depends on elevation and A_{forest} depends on rainfall erosivity, slope-length, slope steepness and soil erodibility. In the catchment scale, when we compare these values, they are well fit as expected (**Fig.10**).

$$A_{forest} = 0.48 \times E_{forest} - 143.70 \quad \text{with } r^2 = 0.99 \quad (21)$$

It means, in the forest area, the erosion from RULSE comprises 48% of erosion from Ohmori's model. In general, if E^* is long-term sheet and rill erosions, eq.(21) can be written as

$$E^* = 0.48 \times E - 143.70 \quad (22)$$

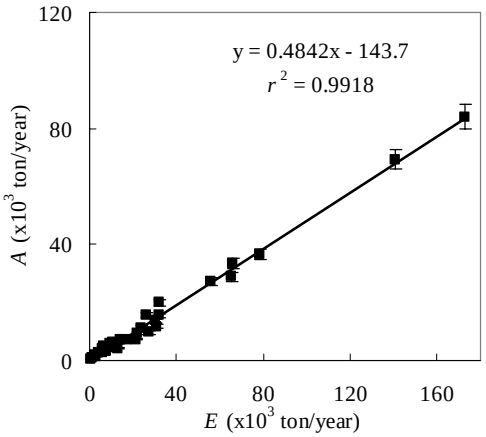

Fig.10 A and E by catchment with stream order 5-7 (n=35).

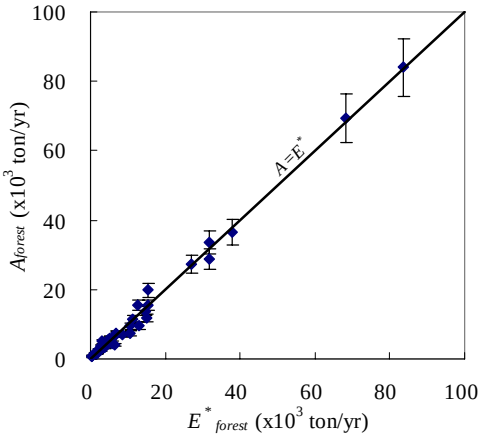

Fig.11 A_{forest} and E^*_{forest} by catchment with stream order 5-7.

5. Discussions

Table 6 shows the results of long-term annual sediment storage calculated from sediment storage in channel, and long-term annual sediment yield calculated from Ohmori's model.

The results show that sediment storage in Onga river basin consists of 47% of total sediment yield (SY). If we can assume that during the time when Onga plain had been a lagoon (8500 years BP), all sediments transported to channels were retained in the basin. It means that the delivery ratio is zero or sediment discharge to channel is equal to storage. Therefore, the sediment discharge to the channels comprises 47% of total sediment yield.

In addition, erosion from eq.(22) comprises 48% of total sediment yield which equals to the sediment storage in whole drainage basin in Holocene. RUSLE model reflects the flows of sediment in and out the cells, and in general, this sediment flows will reach the channels. Oguchi (2001) concluded that almost all the supplied sediments from post glacial hill slope incision were transported directly to piedmont areas and have accumulated on piedmont alluvial fans because of large flood discharge. It means that all sediments yielded from A_{forest} reach to the channel valleys.

Erosion from eq.(19) can be considered the natural erosion without covers and practices. If different CP-values are counted, A-value will also consists of erosions affected by human activities (consider as forestry and agriculture activities), and then, we can assume that erosion due to human activities is extracted by A minus E^* in each catchments.

Table 6 Sediment discharge ratios (SDR) in Onga River Basin in Holocene (8500 years BP).

River basin	stream order	area km^2	storage 10^3 m^3.$year^{-1}$	SY 10^3 m^3.$year^{-1}$	SY to channel 10^3 m^3.$year^{-1}$	SDR (3)-(2)
		(1)	(2)	(3)	(4)	(3)
Miyawaka	6	141.4	4.65	38.53	18.02	0.74
Sub-Iizuka1	6	138.8	5.61	29.02	13.64	0.59
Sub-Iizuka2	6	132.3	5.45	30.25	14.22	0.62
Sub-Tagawa1	6	102.0	3.01	35.12	16.51	0.82
Sub-Tagawa2	6	99.9	3.79	20.53	9.65	0.61
Sub-Tagawa3	6	57.7	1.21	30.68	14.42	0.92
Iizuka	7	383.7	18.85	68.93	32.40	0.42
Tagawa	7	327.3	14.20	102.35	48.10	0.71
Onga basin	8	1036.4	91.61	195.97	92.11	0.0

* Sediment yield (SY), as Ohmori (2003)'s eq.(3). (1) is catchment area; (2) is long-term annual sediment storage; (3) is long-term annual sediment yield; (4) is 47% of (3); and SDR is the Sediment Delivery Ratio.

In **Fig.12**, points above the line have more erosion caused by human activities than by natural erosion (data in **Table 7**). For catchment with stream order 6 and 7, it is clear to recognize the amount of sediment yield by human activities. In two catchments of stream order 7, Iizuka area has higher sediment yield by human activities than Tagawa area, although forest and paddy field area of Iizuka decrease in order to increase urban area with increasing of population. For smaller catchments (**Table 8**), all of catchments 5 with average slope angle over 13.0 degree occur near the line in **Fig.13**, and their sediment yields are within the range of error, but there is one catchment in which the sediment from E is significant higher than A. It can be explained that this catchment located in the fault zone with steepness and high dispersal factor D and denudation process is high magnitude.

Table 7 Erosion of each catchment in forest and agriculture areas (catchment 6&7) [ton/year].

Catchment	A	E^*	A-E^*
	ton/year		
Miyawaka	47964	40329	7634
Sub-Iizuka1	42315	31050	11265
Sub-Iizuka2	42678	34830	7848
Sub-Tagawa1	42708	35111	7597
Sub-Tagawa2	29053	18211	10842
Sub-Tagawa3	21009	23261	-2252
Tagawa	119005	101259	17746
Iizuka	109553	77890	31663
Whole basin	**310093**	**240766**	**69327**

Table 8 Evaluating the errors for catchment 5 [ton/year].

Area	A_{forest}	E_{forest}	Errors (E_{forest}- A_{forest})	A	E^*	E^*-A	Critical	Average slope angle
km^2	ton/year							degree
14.2	7293	10451	3158	9568	10734	1166	Error range	14.8
38.7	11715	15084	3369	15815	15989	173	Error range	14.0
32.9	9466	10660	1194	12893	17138	4245	Abnormal	14.2
10.3	2615	2867	252	3242	3401	159	Error range	13.1
20.6	4544	5849	1305	4993	6271	1278	Error range	15.6
55.1	4096	6452	2356	5230	6715	1484	Error range	13.0
24.6	9609	13107	3498	12024	14328	2304	Error range	13.6

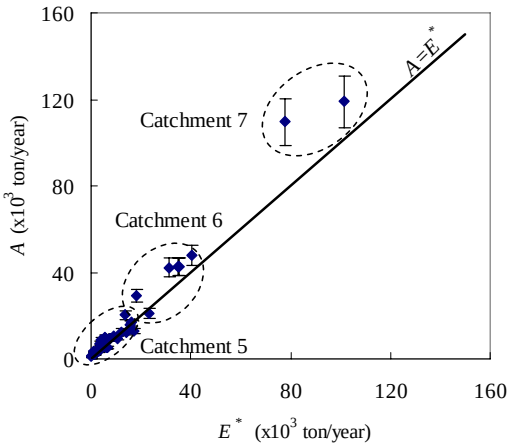

Fig.12 Relation between *A*-*E by catchment 5-7 (error 10%).**

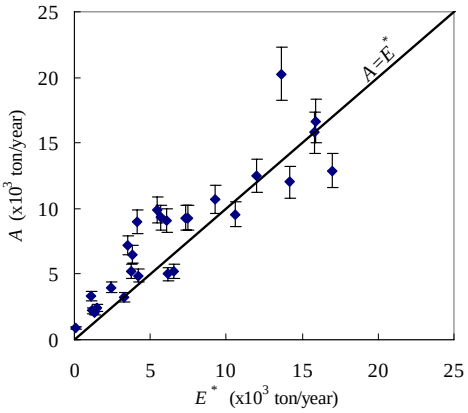

Fig.13 Relation between A-E* by catchment 5 (error 10%).

6. Conclusions

The impact of human activities on erosion is clear in the catchments with stream order 6 & 7, and between the same levels of catchments. The catchments of stream order 5 have average slope angle over 13 degrees, sediment yield from denudation is dominated in comparison with RULSE model.

In Holocene, sediment storage is proportional with area in each catchment of area range from 10 to 1000 km^2. For long-term period, 47% of total erosion discharges to the valley and deposits in the lower part of the basin. Sheet and rill erosions by RUSLE model consist of 48% of total erosion in the basin, or 52 % soil erosion due to slope failures.

Sediment yield from agriculture and forestry is about 69,000 ± 10% tons of soil loss per year. In natural status, Tagawa area yields more sediment than Iizuka area but the storage is lesser, and Iizuka area has higher sediment yield by human activities than Tagawa area. The results are limited in the effects of agriculture and forestry only, other factor as road construction, slope cut, mining, house occupy, etc, aren't accounted.

It can be said that, this is the first time, a relationship between total erosion from denudation model proposed by Ohmori and that of RUSLE model is established in catchment scale in the range of 10 to 1000 km^2.

References

1) P.J.J. Desmet and G. Govers.; A GIS Procedure for Automatically Calculating the USLE LS Factor on Topographically Complex Landscape Units, Journal of Soil and Water cons, Vol. 51, No.5, pp.427-433 (1996).
2) D.K. McCool, G.R. Foster, et al.; Revised Slope Length Factor in the Universal Soil Loss Equation. Trans ASAE, Vol.30, pp.1571-1576 (1989).
3) K.G. Renard and J.R. Freimund; Using Monthly Precipitation Data to Estimate the R-Factor in the Revised USLE. Journal of Hydrology, Vol. 157, pp.287-306(1994).
4) H. Kitahara, Y. Okura, T. Sammori and A. Kawanami.; Application of Universal Soil Loss Equation to Mountainous Forests in Japan. J. For. Res Vol.5, pp.231-236 (2000).
5) S. Yoshikawa, H. Yamamoto, Y. Hanano and A. Ishihara; Hilly-land Soil Loss Equation (HSLE) for Evaluation of Soil Loss Caused by the Abandonment of Agriculture Practices. JARQ vol. 38, pp.21-29 (2004).
6) Y. Taneda; Soil Loss Prediction of a Farm Land in Japan. I.A.H.S. Publ. No. 132 (1981).
7) Y. Taneda; Prediction of Soil Loss in Japan. Stud. Agricultural-land conserve, Vol.1, pp.11-20 (1980) [in Japanese].
8) W.H. Wischmeier and D.D. Smith; Predicting Rainfall Erosion Losses- A Guide to Conservation Planning. USDA, Washington, Argiculture Handbook No.537 (1978).
9) K.G. Renard, G.R. Foster, G.A. Weesies, D.K. MsCool, and D.C. Yoder; Predicting soil erosion by water: A guide to conservation planning with the Revised Universal Soil Loss Equation (RULSE). Argiculture Handbook No.703, USDA, Washington, chapter 3-Soil Erodibility Factor, p.91 (1996).
10) T. Shiono, K. Kamimura, S. Okushima and M. Fukumoto; Soil Loss Estimation on a Local Scale for Soil Conservation Planning. JARQ Vol. 36, No. 3, pp.157-161 (2002).
11) Y. Yokoyama, et al.; Holocene Sea Level Change and Hydro-Isostasy Along the West Coast of Kyushu, Japan. Jour. Palaeography, Palaeoclimatology, Palaeoecology Vol.123, pp.29-47 (1996).
12) Agricultural Structure Improvement Bureau of MAFF; Land Reclamation Designing Diagnosis. Agricultural and Rreclamation, eds, MAFF, Japan, pp. 158-178 (1992) [In Japanese].
13) T. Oguchi, K Saito, H. Kadomura and M. Grossman; Fluvial Geomorphology and Paleohydrology in Japan. Journal of Geomorphology, Vol. 39, pp.3-19 (2001).
14) National Institute for Agro-Environmental Sciences of Japan. Soil Data http://agrimesh.dc.affrc.go.jp/soil_db/index.phtml.
15) G. Einsele; Sedimentary Basins: Evolution, Facies, and Sediment Budget. ISBN: 3-540-66193-x. Springer, 2rd edition, p.454 (2000).
16) T. Hoffmann, G. Erkens, et al.; Holocene Floodplain Sediment Storage and Hill Slop Erosion within the Rhine Catchment. The Holocene, Vol.17, No.1, pp.105-118 (2007).
17) J.P.M. Syvitski, C.J. Vorosmarty, A.J. Kettner and P. Green; Impact of Human on the Flux of Terrestrial Sediment to Global Coastal Ocean. Science, Vol. 308, pp.376-380 (2005).
18) B.Y. Lui, M.A, Nearing, P.J. Shi, and Z.W. Jia; Slope Length Effects on Soil Loss for Steep Slopes. In:D.E. Stott, R.H. Mohtar and G.C. Steinhardt (des). Sustaining the Global Farm. Pp.784-788 (2001).
19) A. Matsubara; Holocene Geomorphologic Development of Coastal Barriers in Japan. Geographical Review of Japan. 73A-5, 409-434 [In Japanese].

20) Counsellor, National and Regional Planning Bureau, Ministry of Land, Infrastructure, Transport and Tourism, Japan. Land-use map in 1997. http://nlftp.mlit.go.jp/ksj/index.html.
21) ESRI. Arc GIS Desktop Help, Interpolation (2007).
22) T. A. Tran, Y. Mitani and H. Ikemi, The relationship between the sediment deposition and catchment characteristics in Onga river basin, Northern Kyushu Island, Japan, Proceedings of International Symposium on a Robust and Resilient Society against Natural Hazards& Environmental Disasters and the Third AUN/SEED-Net Regional Conference on Geo-Disaster Mitigation, pp.248-257 (2010a).
23) T. A. Tran, Y. Mitani, H. Ikemi, and M. Tsukihara, Sediment budget in Holocene: Study case of Onga River basin, Northern Kyushu Island, Japan, Proceedings of the third Regional Conference on Geological Engineering Research in ASEAN (2010b).